DOI: 10.1002/ejic.200800250

On the Role of Tyrosine as Catalytic Base in Nitrile Hydratase

Kathrin H. Hopmann[a][‡] and Fahmi Himo*[a]

Keywords: Nitrile hydratase / Enzyme catalysis / Density functional theory / Reaction mechanism

Nitrile Hydratases (NHases) catalyze the conversion of nitriles to their corresponding amides. Two NHase classes exist, the Fe^{III}-NHases and the Co^{III}-NHases. Both harbour an intriguing active site, with a low-spin metal ion coordinated to deprotonated back-bone amides and oxidized cysteine residues. So far it has not been possible to conclusively determine the reaction mechanism of NHase. Here we employ density functional theory to investigate the recent proposal that a fully conserved second-shell tyrosine residue is the catalytic base of nitrile hydratase (*J. Biol. Chem.* **2007**, *282*, 7397–7404). In the proposed mechanism, the tyrosine is suggested to be in the tyrosinate state and to mediate nitrile hydration through activation of a water molecule, which attacks the metal-bound substrate. We have explored this mechanism employing quantum chemical active site models on the basis of the Co^{III}-NHase from *P. thermophila* JCM 3095 and the Fe^{III}-NHase from *R. erythropolis* N-771. Potential energy curves and optimized transition states are presented. The computed barriers for the two models are a few kcal/mol above the experimental value, indicating that the conserved second-shell tyrosine could function as the catalytic base of NHase. To further evaluate the likelihood of this mechanism, we estimated the pK_a value of the second-shell tyrosine in each model. We also provide estimates of the energy involved in the exchange of a metal-bound water molecule with a nitrile substrate.

I. Introduction

Nitrile hydratases (NHases, EC 4.2.1.84) catalyze hydration of nitriles to give amides (Scheme 1). They are generally divided into two different classes, the non-heme Fe^{III}-NHase and the non-corrinoid Co^{III}-NHase. The latter class is utilized in the industrial production of acrylamide, which amounts to more than 30000 tons annually.[1]

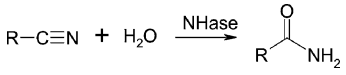

Scheme 1. Nitrile hydration reaction catalyzed by NHase.

The X-ray crystal structures of various NHases revealed a peculiar conserved active site.[2–8] The octahedrally coordinated metal ion has two deprotonated backbone amides as ligands as well as three cysteine residues, two of which are posttranslationally oxidized to cysteine-sulfenic and cysteine-sulfinic acids.[3] The biological significance of these oxidations is to date not known. The sixth metal–ligand of the active NHase remains elusive. It is generally suggested to be a hydroxide ion, a water molecule, or possibly the substrate.[2,4,5,7,9]

[a] Department of Theoretical Chemistry, School of Biotechnology, Royal Institute of Technology,
10691 Stockholm, Sweden
E-mail: himo@theochem.kth.se
[‡] Present address: Centre for Theoretical and Computational Chemistry, Department of Chemistry, University of Tromsø,
9037 Tromsø, Norway

Over the recent years, there have been multiple attempts to synthesize biomimetic complexes that are able to mimic the NHase reaction, but with little success so far.[10] One serious obstacle is the lack of detailed information about the mechanism of NHase. A number of different possible catalytic mechanisms have been put forward in the literature,[7,10–13] but it has not yet been possible to pinpoint one of these as the correct NHase mechanism.

We have previously used density functional theory to investigate different first- and second-shell mechanisms of NHase.[13,14] Active site models on the basis of the iron-containing NHase from *R. erythropolis* N-771 were employed in these calculations.[3] It was shown that a first-shell mechanism involving deprotonation of the attacking water molecule by the first-shell ligand Cys114-SO^- has a computed barrier of 20.2 kcal/mol (Scheme 2, A).[13] Also two second-shell mechanisms have been investigated, involving either a metal-bound hydroxide ion or the first-shell ligand Cys114-SO^- as nucleophile (Scheme 2, B and C).[14] The computed barriers for these two mechanisms were 22.7 and 22.2 kcal/mol, respectively. The barrier for NHase-mediated nitrile conversion is expected to lie in the range of 13–15 kcal/mol (experimental rates are converted employing transition-state theory).[4,8,15] All three computed mechanisms thus exhibit barriers, which are 5–7 kcal/mol above the experimental value. At this point it is thus not possible to identify any of these three mechanisms as the correct NHase mechanism.

Very recently, a novel first-shell mechanism of NHase has been put forward by Mitra and Holz. In this mechanism, a

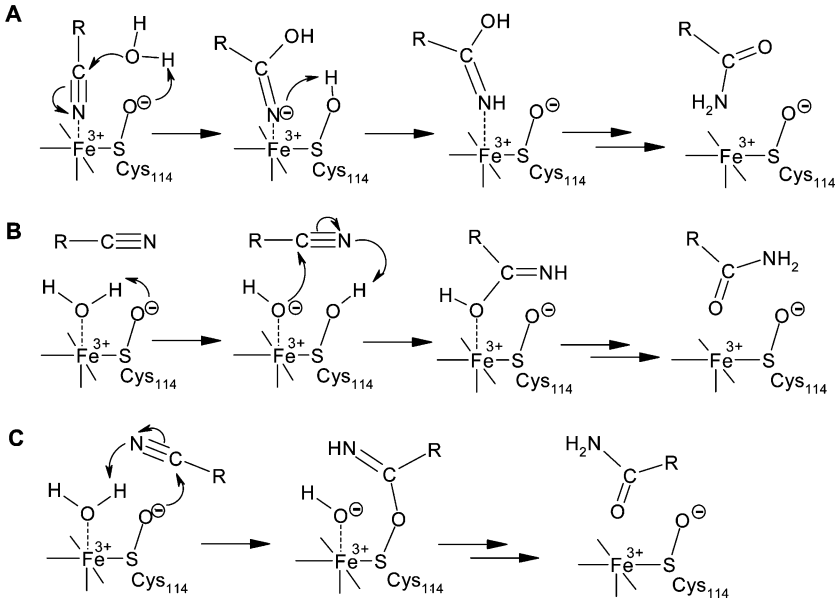

Scheme 2. Previously investigated first- and second-shell mechanisms of Fe^{III}-NHase.[13,14] **A**) First-shell mechanism involving Cys114-SO^- as catalytic base (barrier 20.2 kcal/mol), **B**) Second-shell mechanism employing a metal-bound hydroxide as nucleophile (barrier 22.7 kcal/mol), **C**) Second-shell mechanism employing Cys114-SO^- as nucleophile (barrier 22.2 kcal/mol).

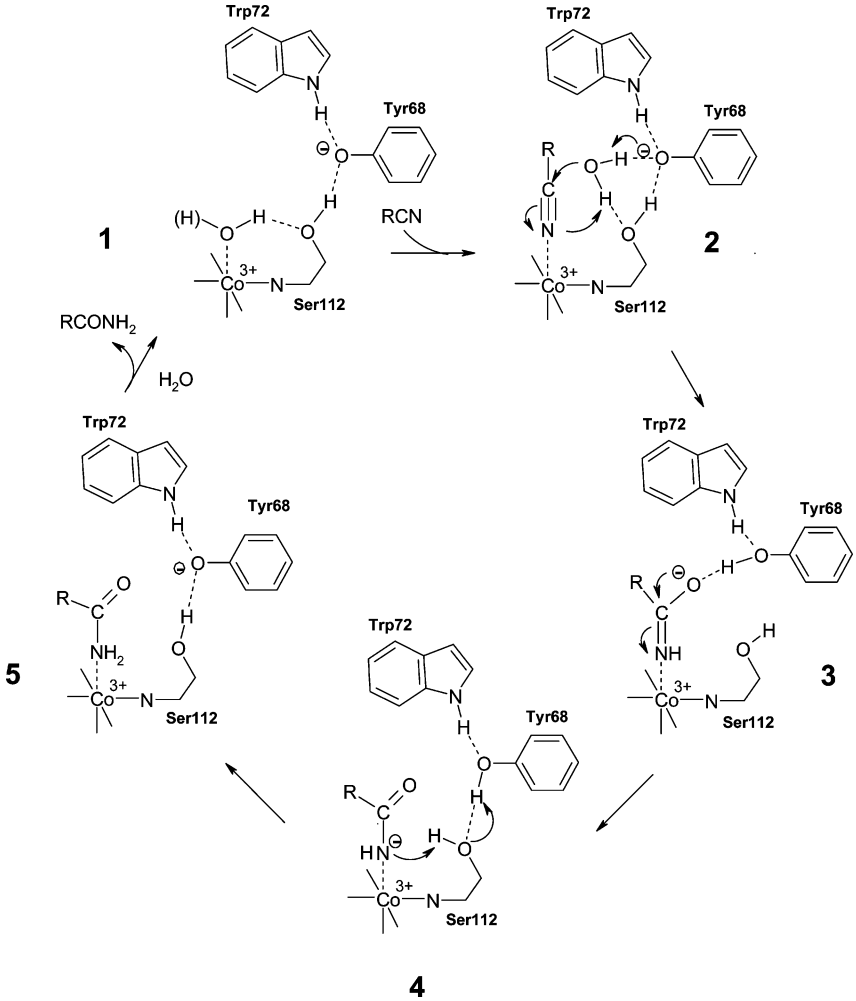

Scheme 3. Proposed first-shell mechanism of Co^{III}-NHase involving Tyr68 as base.[12]

second-shell tyrosine residue is suggested to be the catalytic base of NHase (Scheme 3).[12] This tyrosine is conserved in both the Fe^{III}-NHase and the Co^{III}-NHase (Tyr72 in *R. erythropolis* N-771 Fe^{III}-NHase, Tyr68 in *P. thermophila* JCM 3095 Co^{III}-NHase). Based on experimental results, it was speculated that Tyr68 in the Co^{III}-NHase from *P. thermophila* JCM 3095 might exist in its deprotonated form, stabilized by hydrogen-bonding from the conserved residues Trp72 and Ser112.[12] The deprotonated Tyr68 is proposed to abstract a proton from the nucleophilic water molecule, thus activating it for attack on the metal-bound substrate (Scheme 3).[12]

Here, we use density functional theory to investigate the possibility that the conserved second-shell tyrosine residue is the catalytic base of NHase. Active site models of both the Fe^{III}-NHase and the Co^{III}-NHase were employed to study this proposal. Transition states and barriers for both models are presented. The pK_a value of the conserved second-shell tyrosine is estimated for each model to evaluate the likelihood that it is deprotonated in the NHase active site. Also the energetic cost for exchanging a metal-bound water molecule with a nitrile substrate is estimated.

II. Computational Details

All calculations were performed using the B3LYP functional,[16] as implemented in the Gaussian03 program package.[17] Geometry optimizations were performed using the LANL2DZ basis set. Certain atoms in the active site models were fixed to their crystallographically observed positions during optimizations to preserve the spatial arrangement of the active site model (fixed atoms are marked with asterisks in all figures). Solvation corrections were calculated by performing single point calculations on the optimized geometries using the conductor-like polarizable continuum model (CPCM).[18] Different dielectric constants were employed in these calculations, as discussed in the text. Frequency calculations were performed on all optimized geometries to obtain zero-point vibrational (ZPV) energies and to verify the nature of the optimized stationary points. The freezing scheme employed in calculations results in a few small imaginary frequencies for the optimized geometries. These are on the order of –5 to –20 cm^{-1} and do not influence the results significantly. Final energies were calculated by performing single-point calculations on the optimized geometries at the B3LYP/6-311+G(2d,2p) level.

III. Active Site Models

Two quantum chemical active site models were employed to study a reaction mechanism involving the second-shell tyrosine residue as base. The first model is based on the X-ray crystal structure of the Co^{III}-NHase from *P. thermophila* JCM 3095 (PDB 1IRE[2]) and includes the low-spin cobalt atom ($S = 0$), the first-shell ligands Cys108, Cys111-SO_2^-, Ser112, Cys113-SO^-, and the second-shell ligands Arg52, Arg157, Tyr68 and Trp72 (Figure 1, A). Tyr68 was modeled as phenolate. Residues were truncated and points of truncation were kept fixed to their crystallographically observed positions during geometry optimizations.

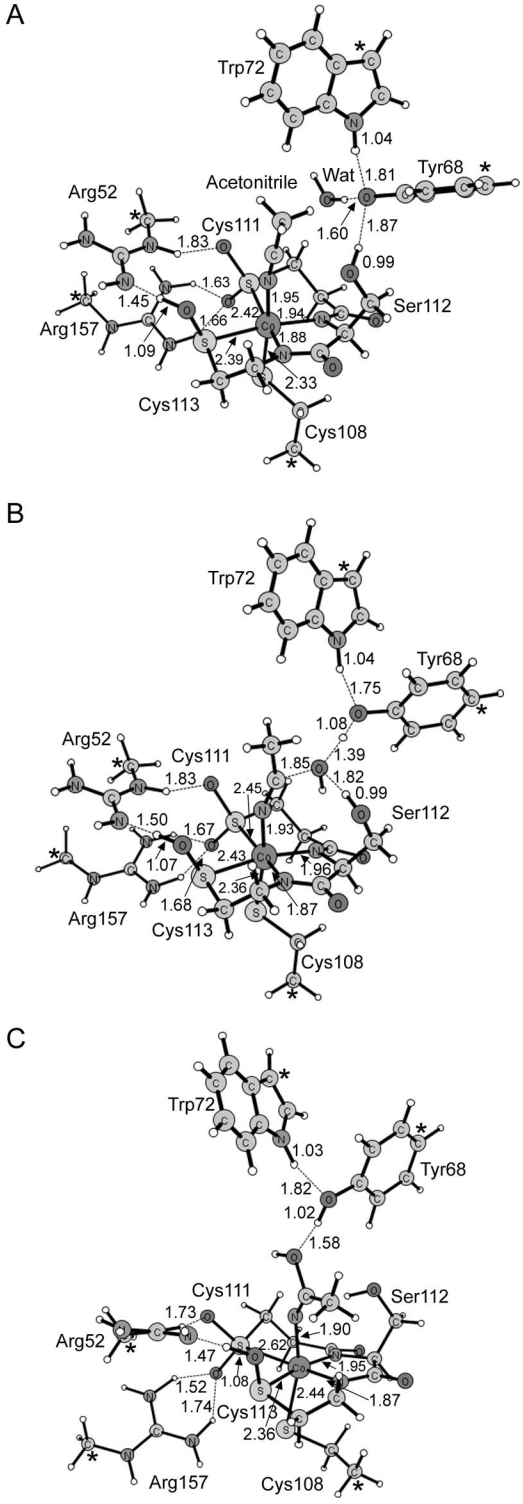

Figure 1. Optimized geometries for Co^{III}-NHase-mediated hydration of acetonitrile with Tyr68 as catalytic base. Distances are in Å. Asterisks mark atoms kept fixed to their crystallographically observed positions during geometry optimizations. **A**) Reactant, **B**) Transition state, **C**) Intermediate.

The second model is analogous to the first model, but is based on the X-ray crystal structure of the Fe^{III}-NHase from *R. erythropolis* N-771 (PDB 2AHJ).[3] The model includes the low-spin iron atom (S = 1/2) and the same first- and second-shell ligands as above, except for Trp72. In the iron-dependent NHase, this residue is replaced by a conserved tyrosine (Tyr76),[2] which instead was included in the model (Figure 2, A).

Acetonitrile was used as substrate in both models, and was placed in the sixth coordination site of the metal ion. Also a water molecule was included in each model and was placed in hydrogen-bonding distance to the second-shell tyrosine as proposed in the above mechanism (Scheme 3, **2**).[12]

The energies for exchanging a metal-bound water molecule with the acetonitrile substrate were computed with slightly reduced active site models. Both the Fe^{III}-NHase and Co^{III}-NHase model employed for computing ligand exchange energies contain all first-shell ligands and the two second-shell arginine residues (Figure 4).

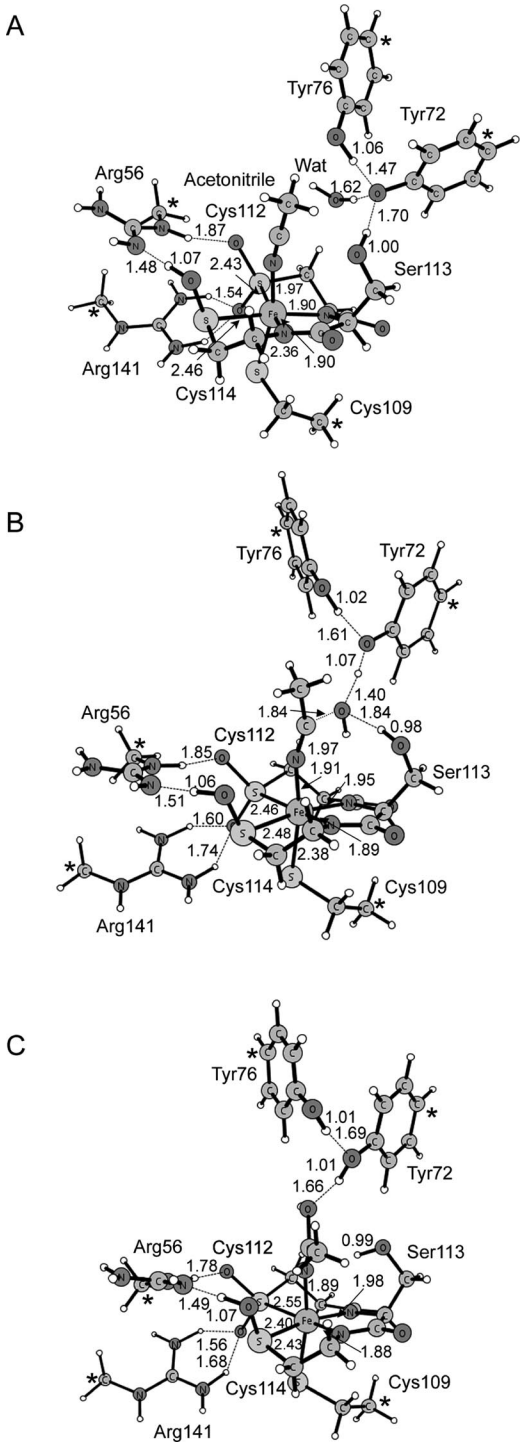

Figure 2. Optimized geometries for Fe^{III}-NHase-mediated hydration of acetonitrile with Tyr72 as catalytic base. **A**) Reactant, **B**) Transition state, **C**) Intermediate.

IV. Results

IV.A. Reaction Mechanism Involving Second-Shell Tyrosine as Base

The optimized active site model of the Co^{III}-NHase with acetonitrile coordinated to the metal ion is shown in Figure 1, A. This structure was taken as the starting point for our investigation of a reaction mechanism involving tyrosine as base. The coordination of the first-shell ligands to the cobalt ion is similar to the previously studied Fe^{III}-NHase active site model (see also below, Figure 2, A).[13,14] The cobalt ion interacts with the deprotonated backbone amides of Ser112 and Cys113 and the three sulfur ligands, Cys108, Cys111 and Cys113. The nitrile substrate is coordinated to the 6th ligand site of the metal, with a nitrogen–cobalt distance of 1.95 Å. In the second shell, the two arginine residues interact with the oxidized side chains of Cys111-SO_2^- and Cys113-SO^-. The two cysteines were both modeled in their ionized state, but during optimization of the reactant structure, a proton was transferred from Arg157 to the Cys113-sulfenate (Figure 1, A). This transfer was also observed in previous NHase active site models,[9,13] and is not likely to influence the obtained results. The second-shell Tyr68 residue is ionized and forms hydrogen bonds with Trp72, Ser112, and the water molecule.

The optimized transition state for the first step of the acetonitrile hydration in the Co^{III}-NHase model comprises a concerted attack of water on the nitrile substrate, and a proton transfer from water to Tyr68 (Figure 1, B). The barrier for this step is computed to 20.6 kcal/mol without solvation corrections (Table 1). At the transition state, the distance between the attacking water molecule and the nitrile carbon is 1.85 Å. One water proton is partially transferred to Tyr68 and is located 1.39 Å from the water oxygen and 1.08 Å from the Tyr68 oxygen (Figure 1, B). The Ser112 side chain interacts with the transient hydroxide ion, thus stabilizing the transition state. Note that the proposed simultaneous transfer of the second water proton to the nitrile nitrogen (Scheme 3, **2**) sterically is not possible. The intermediate formed following water attack is thus protonated at the oxygen atom (Figure 1, C) and has one formal

negative charge on the nitrogen. The protonated Tyr68 interacts with the iminol hydroxy group, but the hydrogen bond between Ser112 and the iminol oxygen atom has been broken. The computed energy of this intermediate relative to the reactant structure is +12.5 kcal/mol without solvation corrections (Table 1).

Table 1. Effect of dielectric constant on the computed energies (kcal/mol) for nitrile hydration employing a first-shell mechanism with tyrosine as catalytic base.

	Fe^{III}-NHase		Co^{III}-NHase	
	Barrier	Reaction energy	Barrier	Reaction energy
No solvation	19.7	17.9	20.6	12.5
ε = 2	18.6	17.2	20.7	14.7
ε = 4	18.0	16.8	20.9	16.1
ε = 8	17.6	16.7	20.9	16.9
ε = 20	17.4	16.6	21.0	17.5
ε = 80	17.3	16.5	21.0	17.7

We have previously shown that the first step in nitrile hydration, nucleophilic attack of water on the substrate to form the iminol intermediate, is the rate-limiting step.[13] The subsequent steps, involving proton transfer to the intermediate to form the neutral iminol and tautomerization to the amide, are thus not studied explicitly here.

The mechanism computed for the Co^{III}-NHase active site model was also studied with the active site model of the Fe^{III}-NHase. As discussed above, the first- and second-shell residues included in the two models are identical except for Trp72, which is replaced by Tyr76 in the Fe^{III}-NHase. The optimized reactant of the Fe^{III}-NHase active site model is shown in Figure 2, A. The interactions and distances in the Fe^{III}-NHase model are similar to the Co^{III}-NHase model. One significant difference is the hydrogen bond formed between the tyrosinate (Tyr72) and Tyr76. The Tyr76 proton exhibits an increased bond length (1.06 Å) and forms a strong hydrogen bond with the Tyr72 oxyanion (proton–oxyanion distance of 1.47 Å, Figure 2, A). In the Co^{III}-NHase, the interaction between the tyrosinate and the Trp72 side chain is much weaker, with a proton–oxyanion distance of 1.81 Å (Figure 1, A).

The optimized transition state for water attack and proton transfer in the Fe^{III}-model is very similar to the cobalt model (Figure 2, B). The critical carbon–oxygen distance is 1.84 Å (compared to 1.85 Å in the Co^{III}-model). The water proton is located between the water oxygen and the tyrosinate, with distances of 1.40 and 1.07 Å, respectively (Figure 2, B). The side chain of Ser113 stabilizes the transient hydroxide, as above. The computed barrier for this transition state is 19.7 kcal/mol without solvation corrections, which is also very similar to the Co^{III}-model (Table 1).

The Fe^{III}-NHase iminol intermediate exhibits a similar configuration as in the Co^{III}-NHase model (Figure 2C). The computed relative energy of the Fe^{III}-NHase iminol intermediate is 17.9 kcal/mol, which is a few kcal/mol higher than the corresponding intermediate in the Co^{III}-model (12.5 kcal/mol, Table 1).

The barriers and reaction energies reported above correspond to the energies computed for the cluster model without solvent corrections. We have computed the effect of the protein surroundings on the energetics of nitrile hydration by employing the conductor-like polarizable continuum model CPCM.[18] A typical dielectric constant used for protein modeling is $\varepsilon = 4$, which is suggested to roughly corresponds to a mixture of protein (dielectric constant: 2–3) and water (dielectric constant of 80).[19] This value was also employed in our previous studies on the first- and second-shell mechanism of NHase.[13,14] However, Richards and coworkers have pointed out that in the X-ray crystal structures of NHase, the active site is easily accessible to water, making it likely that it is well solvated.[9] They therefore suggest to employ a somewhat larger dielectric constant of $\varepsilon = 20$ in calculations on NHase.

We have here tested the effect of the dielectric constant on the barrier for nitrile hydration with the above mechanism (Table 1). For the Fe^{III}-NHase model, the barrier decreases from 19.7 kcal/mol without solvation to 18.0 kcal/mol at $\varepsilon = 4$. If $\varepsilon = 20$ is used instead, an additional reduction of 0.6 kcal/mol is observed. The energy of the intermediate is reduced from 17.9 kcal/mol without solvation to 16.8 kcal/mol at $\varepsilon = 4$ and 16.6 kcal/mol at $\varepsilon = 20$. In the Co^{III}-NHase model, the solvent effect increases the barrier slightly. Employing $\varepsilon = 4$, the increase is only 0.3 kcal/mol, and an additional increase of 0.1 kcal/mol is observed if $\varepsilon = 20$ is employed. The effect on the reaction energy is somewhat larger in the Co^{III}-model. The energy of the intermediate changes from +12.5 kcal/mol without solvation to +16.1 kcal/mol at $\varepsilon = 4$ and +17.5 at $\varepsilon = 20$. The results show that the choice of dielectric constant has very little influence on the barrier for nitrile hydration.

The energies computed for the Fe^{III}-NHase and Co^{III}-NHase models indicate that the second-shell tyrosine could act as the catalytic base of nitrile hydratase. The barriers for both models are somewhat above the experimental value (estimated to 13–15 kcal/mol), but are in both cases so close that a mechanism of this kind cannot be excluded. To further evaluate the likelihood of this mechanism, we analyzed the proton affinity of the second-shell tyrosine. This should indicate if the second-shell tyrosine residue is likely to be deprotonated in the NHase active site. In addition, we also studied the energy involved in replacement of a metal-bound water molecule by the nitrile substrate. This might be a necessary first step in a first-shell mechanism as the one studied here.

IV.B. Proton Affinity of the Second-Shell Tyrosinate

The conserved second-shell tyrosine of nitrile hydratase can function as a base only if it is easily deprotonated prior to nitrile hydration. The hydrogen-bonding network around the tyrosine residue could possibly lower its pK_a value, making deprotonation facile. An ionizable group in Co^{III}-NHase from *P. thermophila* JCM 3095 has an experimentally determined pK_a value of 5.8, which has been suggested to correspond to Tyr68.[12] However, it might also be assigned to other ionizable groups, such as the cysteine-sulfenic or -sulfinic acid.

We have computed the proton affinity (*PA*) of the second-shell tyrosinate in the two NHase models to evaluate the likelihood that it exists in a deprotonated form in the NHase active site (Table 2). The *PA* for each tyrosinate was computed by subtracting the energy of an NHase model with neutral tyrosine residue from the energy of the corresponding model with a tyrosinate residue:

$$PA_{\mathrm{NHaseTyrosinate}} = (E_{\mathrm{NHaseTyrosinate}} - E_{\mathrm{NHaseTyrosine}})$$

Table 2. Computed proton affinities (*PA*, kcal/mol) of free phenolate and the tyrosinate residues in the NHase models.

Model	No solvation	ε = 2	ε = 4	ε = 8	ε = 20	ε = 80
Free Phenolate	346.8	321.0	307.6	300.8	296.7	294.6
Fe^{III}-NHase (Tyr72)	323.9	304.9	294.6	289.3	285.9	284.2
Co^{III}-NHase (Tyr68)	324.5	306.1	296.0	290.8	287.5	285.9

The model with tyrosinate corresponds in each case to the reactant structure shown above, Figure 1, A and Figure 2, A. The Fe^{III}-NHase and Co^{III}-NHase models with neutral tyrosine are shown in Figure 3. The two protonated structures are similar. However, the water molecule is seen to occupy slightly different positions in the two models. In the Fe^{III}-NHase model, it forms an additional hydrogen bond to Cys112-SO_2^- (Figure 3, A). In the Co^{III}-NHase model, the second-shell tyrosine is positioned somewhat further away from the metal center and formation of a hydrogen bond between water and Cys111-SO_2^- is thus not possible in this model (Figure 3B).

To evaluate the effect that the hydrogen-bonding network around the tyrosinate has on the proton affinity, we compared it to the *PA* of free phenolate (Table 2). The *PA* of the second-shell tyrosinate is found to be significantly lower than the *PA* of free phenolate, independently of the dielectric constant employed to compute solvent corrections. This indicates that the hydrogen-bonding network in the NHase active site increases the acidity of the second-shell tyrosine. The two NHase models exhibit similar values (Table 2).

The computed proton affinities can be employed to obtain an estimate of the pK_a value of the second-shell tyrosine. The following relationship is used here:

$$pK_a = \frac{\Delta E}{\ln(10)RT}$$

The relative pK_a of the NHase second-shell tyrosine compared to phenol is thus:

$$\Delta pK_a = pK_a(\mathrm{NHaseTyr}) - pK_a(\mathrm{Phenol}) = \frac{\Delta\Delta E}{\ln(10)RT}$$

where:

$$\Delta\Delta E = (E_{\mathrm{NHaseTyrosinate}} - E_{\mathrm{NHaseTyrosine}}) - (E_{\mathrm{Phenolate}} - E_{\mathrm{Phenol}}) = PA_{\mathrm{NHaseTyrosinate}} - PA_{\mathrm{Phenolate}}$$

An estimate of the pK_a of the second-shell tyrosine can therefore be obtained as follows:

$$pK_a(\mathrm{NHaseTyr}) = pK_a(\mathrm{Phenol}) + \frac{PA_{\mathrm{NHaseTyrosinate}} - PA_{\mathrm{Phenolate}}}{\ln(10)RT}$$

The experimentally measured pK_a of phenol in water is 9.9.[20] The computed proton affinity of phenolate employing a dielectric constant of 80 (corresponding to water) is 294.6 kcal/mol. These values were employed in the above relationship in combination with the computed *PA* values for the NHase tyrosinates to give an approximate pK_a value for the second-shell tyrosine (Table 3). The results show that the computed pK_a value is highly dependent on the used dielectric constant. Employing the typical value of $\varepsilon = 4$ to compute solvent corrections for the NHase active site models results in a pK_a value of 9.9 for Tyr72 in the Fe^{III}-NHase model and 11.0 for Tyr68 in the Co^{III}-NHase model. However, employing a dielectric constant of $\varepsilon = 20$ reduces the

Table 3. Computed pK_a values of the conserved second-shell tyrosine in the Fe^{III}-NHase and Co^{III}-NHase models.

Model	No solvation	ε = 2	ε = 4	ε = 8	ε = 20	ε = 80
Fe^{III}-NHase (Tyr72)	31.4	17.5	9.9	6.0	3.5	2.3
Co^{III}-NHase (Tyr68)	31.8	18.3	11.0	7.1	4.7	3.5

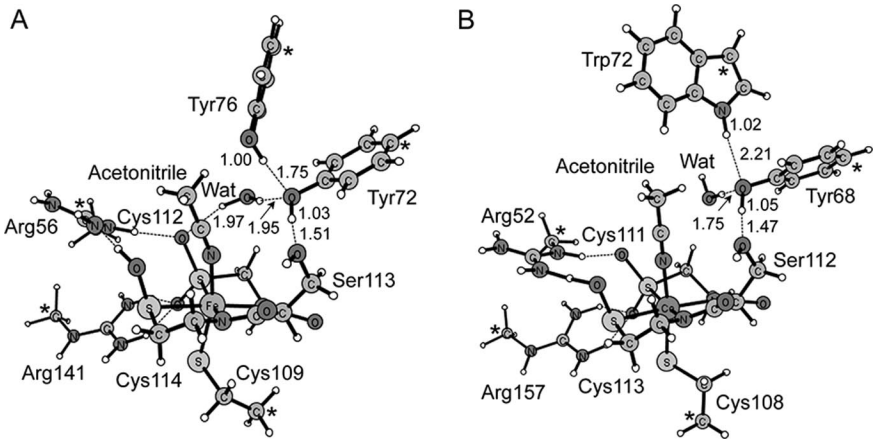

Figure 3. Fe^{III}-NHase (A) and Co^{III}-NHase model (B) with neutral tyrosine residue.

pK_a of Tyr72 to 3.5 and that of Tyr68 to 4.7. The results indicate that it is quite likely that the second-shell tyrosine residue is deprotonated at the NHase active site.

IV.C. Ligand Exchange

An important aspect of the computed first-shell mechanism is the direct coordination of the substrate to the metal ion in the 6th coordination site. It is not clear what ligand normally binds in this site and what the energy involved in displacing it would be. In the inactive form of the iron NHase, an NO molecule is bound in the 6th coordination site.[3] Upon exposure to light, the bond to NO breaks,[21–23] but it is not known, what ligand, if any, replaces the NO. In the X-ray crystal structure of the cobalt NHase a water (or hydroxide) oxygen is observed in the 6th ligand site.[2] This supports the possibility that water is the 6th ligand.

If water is indeed the sixth ligand of NHase, then it is of interest to compute the cost of displacing it by a substrate molecule. Greene and Richards have previously calculated the cost of exchanging a metal-bound water molecule for acetonitrile in a quantum-chemical Fe^{III}-NHase active site model.[9] A thermodynamic cycle was computed, in which the acetonitrile substrate was moved from an aqueous environment to the active site, where it replaced the metal-bound water, which was released to the bulk. This replacement has a computed cost of +7.2 kcal/mol (B3LYP/LACV3P++ energies, including zero-point energies, thermal corrections, and solvation free energies. A dielectric constant of ε = 20 was used for computing solvent corrections for active site models).[9]

We have performed similar calculations here for both a Co^{III}-NHase and an Fe^{III}-NHase active site model. The models are slightly smaller than the models discussed above and do not contain the second-shell tyrosine. The Fe^{III}-NHase model employed in the ligand exchange calculations is shown in Figure 4 (the Co^{III}-NHase model is very similar). The cost of ligand exchange was computed by calculating the energy change in going from an active site model with water coordinated to the metal ion to an active site model with nitrile coordinated to the metal (Scheme 4). Solvent corrections were computed with a dielectric constant of ε = 80 for acetonitrile and water, implying that they are in aqueous solution. For the active site model we tested different dielectric constants (Table 4).

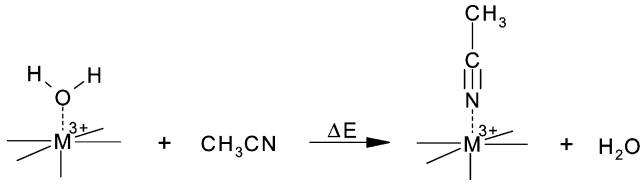

Scheme 4. Exchange of a metal-bound water ligand with acetonitrile.

Table 4. Computed energy (in kcal/mol) of exchanging a metal-bound water molecule with acetonitrile.

Model	No solvation	ε = 2	ε = 4	ε = 8	ε = 20	ε = 80
Fe^{III}-NHase	–4.2	0.9	3.9	5.5	6.5	7.0
Co^{III}-NHase	–4.5	0.1	2.7	4.3	5.1	5.6

The results show that the ligand-exchange energy is dependent on the choice of the dielectric constant. As the dielectric constant is increased, the cost of ligand exchange is raised. For the Fe^{III}-model it is 3.9 kcal/mol at ε = 4 and 6.5 kcal/mol at ε = 20. The latter value is similar to the value computed by Greene and Richards.[9] For the Co^{III}-NHase model, the same trend is observed, although the overall cost is lower. At ε = 4, the cost of ligand exchange is 2.7 kcal/mol, while at ε = 20, it has increased to 5.1 kcal/mol.

The results of the model calculations indicate that the cost of ligand exchange will be in the range of 3–7 kcal/mol. If the sixth metal ligand of NHase is indeed a water molecule, which has to be replaced by the substrate prior to nitrile hydration, then this energy has to be added to the overall barrier.

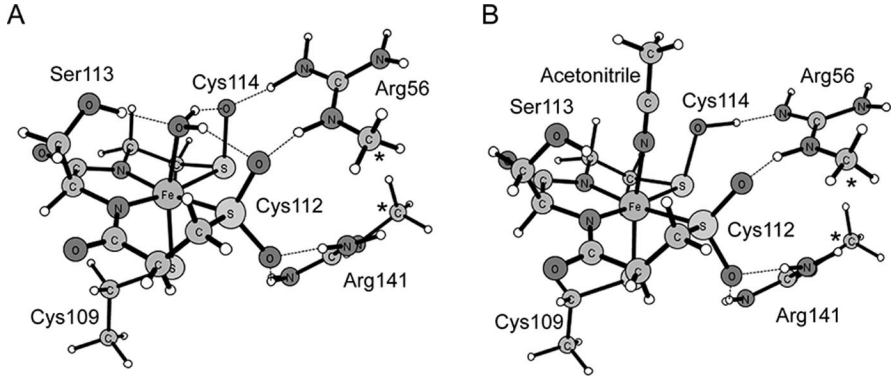

Figure 4. Fe^{III}-NHase active site model employed in ligand-exchange calculations. **A**) Model with metal-coordinated water, **B**) Model with metal-coordinated acetonitrile.

V. Discussion and Conclusions

Our result show that a mechanism involving tyrosinate as base has a barrier that is only a few kcal/mol above the experimental value. Experimental rate constants indicate a barrier of 13–15 kcal/mol for NHase (experimental rates are converted to barriers using classical transition-state theory).[4,8,15] In our calculations, the barrier for nitrile hydration is between 17 and 21 kcal/mol, depending on the employed dielectric constant. For systems containing transition metals, B3LYP has an estimated error on relative energies of 3–5 kcal/mol.[24] Considering this error margin, the computed barriers indicate that the second-shell tyrosine of NHase indeed could be the catalytic base of NHase. However, a number of considerations need to be taken into account. First, it is interesting to evaluate the likelihood that the second-shell tyrosine is in its deprotonated form in the NHase active site. Despite the fact that our calculated pK_a values are very sensitive to the choice of dielectric constant, they show that the second-shell tyrosine might be in the deprotonated state. This would allow the second-shell tyrosine to function as catalytic base.

If NHase employs a first-shell mechanism, then a possible cost for ligand exchange has to be paid to allow the substrate to coordinate to the metal center. In our calculations, the computed cost of exchanging a metal-bound water molecule with acetonitrile in the two active site models is in the range of 3–7 kcal/mol, depending on the employed dielectric constant. This energy will contribute to increase the overall barrier of the reaction. However, the increase is not so high that a first-shell mechanism of the kind studied here can be excluded.

The overall results thus do not exclude the possibility that the second-shell tyrosine is the catalytic base of NHase. However, an important objection to this proposal has to be discussed here. Mutation of Tyr68 in *P. thermophila* JCM 3095 to phenylalanine results in a 126-fold decrease in the k_{cat} for acrylonitrile conversion from 1910 s^{-1} to 15.2 s^{-1}.[8] This corresponds to a barrier increase of only 3 kcal/mol, which is much less than one would expect for mutation of a catalytic base that acts in the rate-limiting step of the reaction. For conversion of benzonitrile, the reduction of the k_{cat} of the Tyr68Phe mutant is only 17-fold,[8] corresponding to a barrier increase of less than 2 kcal/mol. Thus, these experimental results indicate that Tyr68 is not essential for NHase-mediated nitrile conversion. The small barrier increases are more consistent with a role as stabilizing residue, i.e. donation of a hydrogen bond to the substrate or another catalytic residue. The second-shell tyrosine could also function as a general acid, promoting protonation of the substrate, for example after formation of a metal-bound intermediate (such as suggested in Scheme 3, **4**).

Acknowledgments

We gratefully acknowledge financial help from the Swedish Research Council, the Wenner-Gren Foundations, the Carl Trygger Foundation, and the Magn Bergvall Foundation.

[1] A. S. Bommarius, B. R. Riebel, *Biocatalysis*, **2004**, Wiley-VCH, Weinheim, Germany.
[2] A. Miyanaga, S. Fushinobu, K. Ito, T. Wakagi, *Biochem. Biophys. Res. Commun.* **2001**, *288*, 1169–1174.
[3] S. Nagashima, M. Nakasako, N. Dohmae, M. Tsujimura, K. Takio, M. Odaka, M. Yohda, N. Kamiya, I. Endo, *Nat. Struct. Biol.* **1998**, *5*, 347–351.
[4] H. Takarada, Y. Kawano, K. Hashimoto, H. Nakayama, S. Ueda, M. Yohda, N. Kamiya, N. Dohmae, M. Maeda, M. Odaka, *Biosci. Biotechnol. Biochem.* **2006**, *70*, 881–889.
[5] S. Hourai, M. Miki, Y. Takashima, S. Mitsuda, K. Yanagi, *Biochem. Biophys. Res. Commun.* **2003**, *312*, 340–345.
[6] M. Tsujimura, N. Dohmae, M. Odaka, M. Chijimatsu, K. Takio, M. Yohda, M. Hoshino, S. Nagashimai, I. Endo, *J. Biol. Chem.* **1997**, *272*, 29454–29459.
[7] W. Huang, J. Jia, J. Cummings, M. Nelson, G. Schneider, Y. Lindqvist, *Structure* **1997**, *5*, 691–699.
[8] A. Miyanaga, S. Fushinobu, K. Ito, H. Shoun, T. Wakagi, *Eur. J. Biochem.* **2004**, *271*, 429–438.
[9] S. N. Greene, N. G. J. Richards, *Inorg. Chem.* **2006**, *45*, 17–36.
[10] J. A. Kovacs, *Chem. Rev.* **2004**, *104*, 825–848.
[11] M. Kobayashi, S. Shimizu, *Nat. Biotechnol.* **1998**, *16*, 733–736.
[12] S. Mitra, R. C. Holz, *J. Biol. Chem.* **2007**, *282*, 7397–7404.
[13] K. H. Hopmann, J. D. Guo, F. Himo, *Inorg. Chem.* **2007**, *46*, 4850–4856.
[14] K. H. Hopmann, F. Himo, *Eur. J. Inorg. Chem.* **2008**, 1406–1412.
[15] F. Alfani, M. Cantarella, A. Spera, P. Viparelli, *J. Mol. Catal. B* **2001**, *11*, 687–697.
[16] a) C. Lee, W. Yang, R. G. Parr, *Phys. Rev. B* **1988**, *37*, 785–789; b) A. D. Becke, *Phys. Rev. A* **1988**, *38*, 3098–3100; c) A. D. Becke, *J. Chem. Phys.* **1992**, *96*, 2155–2160; d) A. D. Becke, *J. Chem. Phys.* **1992**, *97*, 9173–9177; e) A. D. Becke, *J. Chem. Phys.* **1993**, *98*, 5648–5652.
[17] *Gaussian 03*, M. J. Frisch et al., Gaussian, Inc., Wallingford CT, **2004**.
[18] a) A. Klamt, G. Schüürmann, *J. Chem. Soc. Perkin Trans. Trans. 2* **1993**, *2*, 799–805; b) J. Andzelm, C. Kölmel, A. Klamt, *J. Chem. Phys.* **1995**, *103*, 9312–9320; c) V. Barone, M. Cossi, *J. Phys. Chem. A* **1998**, *102*, 1995–2001; d) M. Cossi, N. Rega, G. Scalmani, V. Barone, *J. Comput. Chem.* **2003**, *24*, 669–681.
[19] P. E. M. Siegbahn, M. R. A. Blomberg, *Chem. Rev.* **2000**, *100*, 421–437.
[20] E. S. Andersen, H. Parbo, *Kemi i perspektiv 2*, **1990**, 2ed., Nordisk forlag A. S., Copenhagen, Denmark.
[21] T. Noguchi, J. Honda, T. Nagamune, H. Sasabe, Y. Inoue, I. Endo, *FEBS Lett.* **1995**, *358*, 9–12.
[22] I. Endo, M. Nojiri, M. Tsujimura, M. Nakasako, S. Nagashima, M. Yohda, M. Odaka, *J. Inorg. Biochem.* **2001**, *83*, 247–253.
[23] I. Endo, M. Odaka, M. Yohda, *Trends Biotechnol.* **1999**, *17*, 244–248.
[24] P. E. M. Siegbahn, *J. Biol. Inorg. Chem.* **2006**, *11*, 695–701.

Received: March 10, 2008
Published Online: July 4, 2008

